


RESEARCH

Open Access



# Ameliorative effects of mesenchymal stromal cells on senescence associated phenotypes in naturally aged rats

Lu Wang<sup>1,2,3†</sup>, Zihui Deng<sup>4†</sup>, Yun Li<sup>1,2†</sup>, Yiqi Wu<sup>1,2</sup>, Renqi Yao<sup>5</sup>, Yuan Cao<sup>1,6</sup>, Min Wang<sup>1,2</sup>, Feihu Zhou<sup>1,3</sup>, Hanyu Zhu<sup>2,3,7\*</sup> and Hongjun Kang<sup>1,2,3\*</sup> 

## Abstract

**Background** Aging is a multifaceted process that affects all organ systems. With the increasing trend of population aging, aging-related diseases have resulted in significant medical challenges and socioeconomic burdens. Mesenchymal stromal cells (MSCs), due to their antioxidative stress, immunoregulatory, and tissue repair capabilities, hold promise as a potential anti-aging intervention.

**Methods** In this study, we transplanted MSCs into naturally aged rats at 24 months, and subsequently examined levels of aging-related factors such as  $\beta$ -galactosidase, superoxide dismutase, p16, p21 and malondialdehyde in multiple organs. Additionally, we assessed various aging-related phenotypes in these aged rats, including immune senescence, lipid deposition, myocardial fibrosis, and tissue damage. We also conducted a 16 S ribosomal ribonucleic acid (rRNA) analysis to study the composition of gut microbiota.

**Results** The results indicated that MSCs significantly reduced the levels of aging-associated and oxidative stress-related factors in multiple organs such as the heart, liver, and lungs of naturally aging rats. Furthermore, they mitigated chronic tissue damage and inflammation caused by aging, reduced levels of liver lipid deposition and myocardial fibrosis, alleviated aging-associated immunodeficiency and immune cell apoptosis, and positively influenced the gut microbiota composition towards a more youthful state. This research underscores the diverse anti-aging effects of MSCs, including oxidative stress reduction, tissue repair, metabolic regulation, and improvement of immune functions, shedding light on the underlying anti-aging mechanisms associated with MSCs.

**Conclusions** The study confirms that MSCs hold great promise as a potential anti-aging approach, offering the possibility of extending lifespan and improving the quality of life in the elderly population.

**Keywords** Anti-aging, Mesenchymal stromal cells, Oxidative stress, Lipidation, Gut microbiota

<sup>†</sup>Lu Wang, Zihui Deng and Yun Li contributed equally to this work.

\*Correspondence:

Hanyu Zhu

hanyuzhu301@126.com

Hongjun Kang

doctorkang301@163.com

Full list of author information is available at the end of the article



## Background

Senescence is a fundamental transformation that occurs in the human body throughout its lifespan, characterized by the loss of youthful traits and the acquisition of deleterious characteristics [1]. As of 2019, the global population aged 65 and above reached 702.9 million, and projections suggest that by 2050, this number will escalate to 1.5489 billion, constituting one-sixth of the world's population [2]. The increasing elderly population is accompanied by a rise in the prevalence of aging-related diseases such as atherosclerosis, hypertension, neurodegenerative disorders, and cancer, imposing significant medical and socio-economic burdens [3]. Aging is a complex process that can affect all organs [4], and it involves various cell-autonomous events known as “hallmarks of aging,” including genomic instability, metabolic aberrations, stem cell exhaustion, and the accumulation of senescent cells [5]. It is widely accepted that the continuous generation of free radicals during cellular metabolism plays a central role in inducing human aging [6]. Moreover, dysregulation of oxidative stress responses leads to persistent subclinical inflammatory states, cellular senescence, and tissue damage in various organs [3], such as the central nervous system's neurodegenerative disorders and cardiac fibrosis. Furthermore, aging results in systemic metabolic dysfunction, leading to higher incidence rates of diseases like diabetes and obesity with advancing age [7]. Additionally, aging brings about comprehensive immunosenescence, primarily involving dysregulation of immune cells and serum immunological functions, rendering the elderly more susceptible to infections and tumorigenesis [8]. In recent decades, numerous researchers have dedicated their efforts to uncovering anti-aging interventions capable of extending lifespan. Various novel nutritional supplements, pharmaceuticals, dietary or exercise regimens, and other biological therapies have been identified as potential measures to mitigate the progression of aging [9]. However, the characteristics of systemic aging are highly interconnected, and many anti-aging strategies target specific aging processes rather than addressing aging phenotypes in all organs throughout the body [10]. Therefore, an optimal anti-aging approach should possess the ability to concurrently regulate multiple aging processes and improve a range of aging phenotypes.

Mesenchymal stromal cells (MSCs) are versatile progenitor cells with diverse sources, obtainable from various tissues such as bone marrow, adipose tissue, perinatal tissues, and dental tissues [11]. Extensive research has consistently demonstrated that MSCs possess the ability to home to injured tissues, alleviate oxidative stress and inflammatory responses, promote tissue repair, and restore proper immunological functions [12, 13]. These numerous advantageous properties have led to considerable attention being directed towards MSCs in the field of

anti-aging research. Previous studies have indicated that MSCs can regulate oxidative stress responses, leading to the improvement of endothelial cell senescence and the stimulation of angiogenesis [14]. Animal studies have shown that transplanting bone marrow-derived MSCs into mice can extend both their lifespan and healthspan, while also exerting a protective effect against the aging of stem cells and fibroblasts [15]. Additionally, MSCs have been investigated in research on frailty syndromes associated with aging, and Phase I and II clinical trials have validated the safety and efficacy of MSCs in ameliorating aging-related frailty [16]. These findings highlight the significant potential of MSCs to ameliorate various aging-related physiological processes. Nevertheless, it is crucial to recognize that systemic aging is a complex process, with each physiological activity interconnected in an intricate manner. Thus, it becomes imperative to thoroughly investigate the comprehensive regulatory effects of MSCs on aging. This investigation will provide substantial evidence to support the use of MSCs in anti-aging applications.

There have been some previous studies confirming the protective effects of MSCs against aging, but most of them were limited to a certain type of cell or a certain organ damage. However, it is well known that organ aging is not independent in the aging process of the organism, and MSCs do not exert anti-aging effects only on a single organ. The current study comprehensively evaluates the senescent state of aged Sprague-Dawley rats after treatment with umbilical cord-derived mesenchymal stromal cells (UC-MSCs) administered via injection. This evaluation involves measuring the levels of aging factors and oxidative stress markers in various organs. Particular emphasis is placed on age-associated chronic inflammation, myocardial injury, lipid deposition, and immunosenescence. Additionally, the study analyzes changes in the composition of the gut microbiota in the rats before and after treatment, aiming to elucidate the beneficial effect of MSCs on aging-related phenotypes. These findings offer a novel perspective for comprehending the anti-aging functions of MSCs.

## Methods

### Study design

This research involved three distinct groups: a young control group ( $n=5$ ), an aged control group ( $n=5$ ), and an aged treatment group ( $n=5$ ). Once the rats were randomly assigned to their respective groups (based on the random number table method), they underwent weekly tail vein injections of either UC-MSCs or saline, totaling four injections. The aged treatment group received  $5 \times 10^6$  UC-MSCs (dissolved in 1 ml of saline) during each injection, while the young control and aged control groups received equivalent volumes of saline at the

same intervals [17]. Rats were placed in the same position before and after each injection, and injections were performed sequentially by rat number to avoid potential confounders. Before the injections, peripheral blood was collected from the rats in the aged treatment group for flow cytometric analysis. One week after the completion of the fourth injection, fecal samples were collected from each rat. Subsequently, all rats were euthanized via decapitation, and peripheral blood and key organs were preserved for subsequent analysis (Fig. 1-A).

### Experimental animals

The study utilized 10 male Sprague-Dawley rats aged 24 months (weighing  $853.5 \pm 50.5$  g) and 5 male Sprague-Dawley rats aged 8 weeks (weighing  $186.62 \pm 10.58$  g),

which were provided by Sibeifu (Beijing) Biotechnology Co., Ltd (Beijing, China). All rats used in this study were examined for tumors visible on the body surface, and if in vivo tumors were found during sampling, that individual was also excluded. The experimental rats were housed in the Experimental Animal Center of the General Hospital of the People's Liberation Army, in a specific pathogen-free environment, maintained at a constant temperature of 24 °C and 60% relative humidity. They were exposed to a light/dark cycle with alternating 12 h of light and 12 h of darkness, and were provided with unrestricted access to food and water throughout the experiment. All animal procedures were conducted in accordance with the care of experimental animals guidelines outlined by the National Institutes of Health, USA, and were approved by

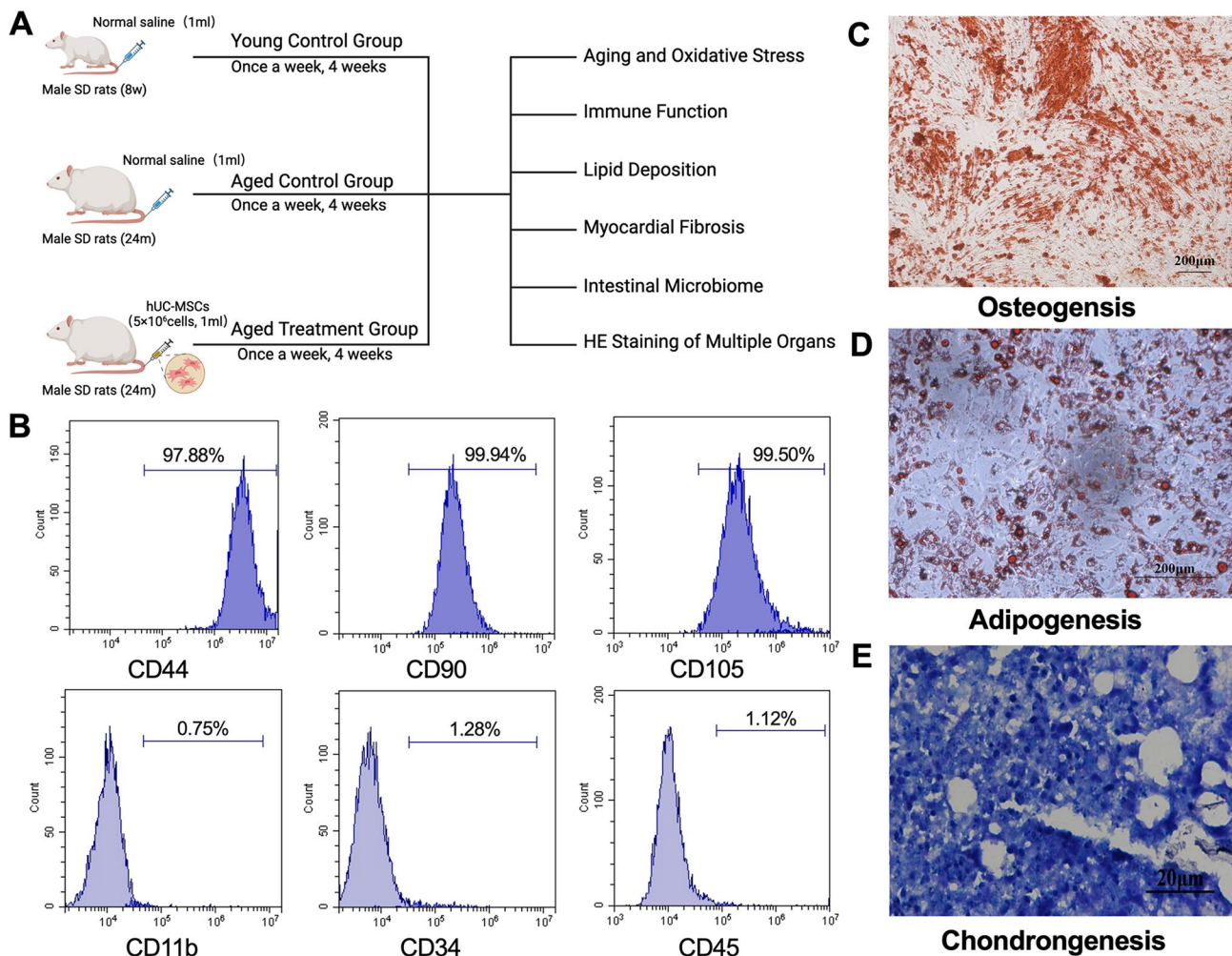


**Fig. 1** Research process and identification of umbilical cord mesenchymal stromal cells. In this study, UC-MSCs are identified through surface markers and their potential for adipogenic, osteogenic, and chondrogenic differentiation. **(A)** The research flow diagram summarizes the experimental animals used in this study, the experimental grouping, treatment methods, and detection techniques. **(B)** Flow cytometry identifies the surface markers of the UC-MSCs cultured and isolated in this study, demonstrating that the proportion of cells positive for CD44, CD90, and CD105 is  $\geq 95\%$ , while the proportion of cells positive for CD11b, CD34, and CD45 is  $\leq 5\%$ . **(C)** Alizarin Red staining identifies the cells' osteogenic differentiation potential. Scale = 200 μm. **(D)** Oil Red O staining identifies the cells' adipogenic differentiation potential. Scale = 200 μm. **(E)** Toluidine Blue staining identifies the cells' chondrogenic differentiation potential. Scale = 200 μm

the Animal Welfare and Ethics Committee of the Chinese PLA General Hospital, China. The sample size used in this study was estimated on the basis of degrees of freedom, totaling 3 subgroups of 15 rats with  $E=12$  consistent with normal values.

#### Isolation, cultivation, and identification of MSCs

Umbilical cords were sourced from the Department of Obstetrics and Gynecology, First Medical Center of the General Hospital of the People's Liberation Army, China. Informed consent was obtained from the mothers who provided the umbilical cords, and this study received approval from the Ethics Committee of the General Hospital of the People's Liberation Army, China. The UC-MSCs were isolated, cultured, and expanded following established protocols [18]. Specifically, UC-MSCs were cultured in minimum essential medium (MEM) medium (Gibco, Thermo Fisher Science, Cat# 12,571,063, MA, USA) supplemented with 10% fetal bovine serum (FBS) (Gibco, Thermo Fisher Science, Cat# 10,099,141, MA, USA). Upon reaching 70–80% confluence, the cells were detached and passaged using trypsin-ethylenediaminetetraacetic acid (EDTA) (Gibco, Cat# 25,300,054). All UC-MSCs used in this study for aging rats were well-growing MSCs derived from passages 3 to 5 (P3–P5).

The identification of UC-MSCs was carried out following previously described methods [17]. Immunophenotyping of the third passage (P3) MSCs was conducted using a flow cytometer. Cells were collected and adjusted to  $5 \times 10^5$  cells per sample, washed with phosphate buffered saline (PBS), and then incubated with antibodies in the dark at room temperature for 15 min. The following antibodies were used from eBioscience, Thermo Fisher Science (MA, USA): PE CD11b monoclonal antibody (Cat# RM2804), PE CD34 monoclonal antibody (Cat# 12-0349-41), APC CD44 monoclonal antibody (Cat# 47-0441-82), APC CD45 monoclonal antibody (Cat# 47-0451-82), APC CD90 monoclonal antibody (Cat# 17-0909-41), and PE CD105 monoclonal antibody (Cat# MA5-17946). Following incubation, the cells were washed with PBS and analyzed using the BD Accuri C6 software system (Version 1.0.264.21; BD Biosciences).

To analyze the differentiation potential of MSCs, the Human Mesenchymal Stem Cell Differentiation Kit (TBDscience, Tianjin, China) was used. P3-MSCs were cultured at a density of  $10^4$  cells/well in a 6-well culture plate, and adipogenic (Cat# TBD20190004), osteogenic (Cat# TBD20190002), and chondrogenic (Cat# TBD20190003) differentiation assays were performed following the kit instructions. After differentiation, the results were observed and photographed under a microscope.

#### Histology and tissue staining

The hearts, livers, lungs, kidneys, intestines, spleens, and brain tissues obtained from the rats in each group were fixed in 4% polyformaldehyde for 24 h, washed, dehydrated, and cleared. Subsequently, the tissues were placed in embedding boxes, and the tissue blocks were trimmed and sectioned (5  $\mu$ m). The sections used for staining were paraffin sections, except for the sections used for oil red O staining, which were frozen sections. The main steps of hematoxylin-eosin (HE) staining involved deparaffinization of the paraffin sections, eosin staining, and dehydration sealing. Nissl staining was performed by deparaffinizing the sections and staining them with methylene blue, followed by gradient alcohol dehydration. For Oil red O staining, the sections were fixed, stained with oil red O working solution, underwent background differentiation, eosin staining, and were then sealed with glycerol gelatin sealing agent. The Masson staining process included deparaffinization of the paraffin sections, staining with Masson's working solution, differentiation with acetic acid, dehydration, and transparent sealing. Wheat germ agglutinin (WGA) staining involved deparaffinization of the paraffin sections, antigen repair, WGA dye staining, DAPI counterstaining of cell nuclei, quenching of tissue autofluorescence, and sealing. The stained sections were visualized and scanned using the Panoramic MIDI CaseViewer system (3DHISTECH, Hungary). The immunohistochemical staining of p16 (Servicebio, Cat# GB11703, China, 1:200) and p21 (Servicebio, Cat# GB15153, China, 1:500) encompassed steps including primary antibody incubation, secondary antibody incubation, washing, hematoxylin nuclear staining, further washing, dehydration, and slide mounting. Antigen repair conditions were: citric acid (pH 6.0) as buffer; microwave at medium heat (850 W) for 8 min; cease fire for 8 min; and microwave at medium-low heat (750 W) for 7 min. The expression of p16 and p21 was evaluated using the H-Score immunohistochemical scoring system, where  $H\text{-Score} = \sum(\pi \times i) = [\text{percentage of cells with weak intensity (grey value of 121–180)} \times 1] + [\text{percentage of cells with moderate intensity (grey value of 61–120)} \times 2] + [\text{percentage of cells with strong intensity (grey value of 0–60)} \times 3]$  [19]. For TdT-mediated dUTP Nick-End Labeling (Tunel) and proliferating cell nuclear antigen (PCNA) staining, after dewaxing and rehydrating the paraffin sections, the appropriate reagents, as per the instructions of the kit, were applied, followed by DAPI counterstaining of the cell nuclei.

#### ELISA detection of aging-related factors levels

After centrifugation, plasma was separated from peripheral blood, and the organs were ground to create cell suspensions. The supernatant obtained after centrifugation was retained. The levels of aging-related factors were

determined using enzyme-linked immunosorbent assay (ELISA) following the instructions of the corresponding kits (Meimian, China). The optical density (OD) values of each well were measured by an ELISA reader at 450 nm (beta-galactosidase ( $\beta$ -gal), lipofuscin (Lipo), immunoglobulin G (IgG), superoxide dismutase (SOD), interleukin-1beta (IL-1 $\beta$ ), IL-6), 532 nm and 600 nm (malondialdehyde (MDA)), and 412 nm (glutathione (GSH)). Based on the OD values, standard curves were constructed, and the levels of  $\beta$ -gal, Lipo, IgG, SOD, MDA, GSH, IL-1 $\beta$ , and IL-6 in the peripheral blood and organs of the rats in each group were calculated.

### Flow cytometry

Approximately 0.5 mL of peripheral blood was collected from each group of rats. To each sample, 10  $\mu$ L of CD3-APC, CD4-FITC, CD8-PE, and CD45-PerCP antibodies (eBioScience, USA) were added. The samples were then incubated at room temperature in the dark for 15 min. Following this, 500  $\mu$ L of red cell lysis solution was added, and the mixture was incubated in the dark for another 15 min before being centrifuged. The supernatant was discarded, and the precipitate was resuspended with 200  $\mu$ L of PBS. The proportions of CD4+ and CD8+ T cells were determined by flow cytometry, and the CD4+/CD8+ T cell ratio was calculated.

### 16 S RNA detection of fecal intestinal microflora

Fresh fecal samples were collected from each rat before sampling. The main steps of the analysis were as follows: (1) Total genomic DNA of microbial communities was extracted, and its quality was checked following the instructions of the DNA extraction kit (Tiangen Biotech, Beijing, China); (2) PCR amplification of the V3-V4 variable region of the 16 S rRNA gene was carried out using the primer sequences in the subsequent table; (3) The purified PCR product was used to construct a sequencing library using the NEXTFLEX Rapid DNA-Seq Kit (Bioo Scientific, Austin, Texas, USA); (4) High-throughput sequencing and data analysis were performed, and operational taxonomic unit (OTU) taxonomic annotation was done by aligning against the Silva 16 S rRNA gene database (v138). Moreover, 16 S functional prediction analysis was conducted using PICRUSt2 (version 2.2.0) software; (5) Finally, statistical analysis was carried out.

Primer	Sequence
338 F	ACTCCTACGGGAGGCAGCAG
806R	GGACTACHVGGGTWTCTAAT

### Statistical analysis

Statistical analysis was performed using SPSS 22.0 software. Measurement data were expressed as  $\bar{x} \pm s$  and were tested for homogeneity of variance. For groups with

equal variance, a one-way analysis of variance (ANOVA) was used for comparisons among multiple groups, followed by the Tukey's post hoc test for further pairwise comparisons between groups. In cases of unequal variance, the Welch's approximate F-test was employed, and Dunnett's T3 method was used for further pairwise comparisons between groups. Statistical graphing was carried out using GraphPad Prism 9.0. A significance level of  $P < 0.05$  was considered statistically significant.

## Results

### Identification of umbilical cord mesenchymal stromal cells

In this study, the UC-MSCs used in the research were assessed to meet international standards through flow cytometry and directed induction differentiation. The results of flow cytometry demonstrated that the expression rates of positive markers CD44, CD90, and CD105 all exceeded 95%, while the expression rates of negative markers CD11b, CD34, and CD45 did not surpass 2% (Fig. 1-B). Upon the addition of the osteogenic induction medium, the microscope observation revealed a reduction in the intercellular gap of UC-MSCs, accompanied by bone calcium deposition, and Alizarin Red staining showed positive results (Fig. 1-C). Likewise, the addition of the adipogenic induction medium led to the observation of round, transparent, tiny lipid droplets in the cells under the microscope. As the culture time extended, the lipid droplets increased in volume and fused, and Oil Red O staining showed positive results (Fig. 1-D). Furthermore, upon adding the chondrogenic induction medium, the microscope observation revealed that the differentiated chondrocytes gathered into groups, and Toluidine Blue staining was positive (Fig. 1-E). The results herein demonstrate that the UC-MSCs employed in this study conform to the identification criteria for MSCs.

### Anti-aging effects of MSCs on peripheral vital organs

The HE results indicated that, the lungs of old rats exhibited expanded alveolar ducts and cavities, atrophied and decreased alveolar epithelial cells, and proliferation of fibrous tissue in the alveolar septum, when compared to the lungs of young rats. In the kidneys of old rats, the glomeruli were enlarged, the number of glomeruli decreased, the endothelial cells in the glomerular capillaries reduced, focal segmental glomerulosclerosis phenomena were observed, renal tubules atrophied, the number of epithelial cells decreased, and renal interstitial fibrosis occurred, in contrast to the kidneys of young rats. Additionally, the intestines of old rats showed changes in the structure of the small intestinal mucosa, including sparse, falling off, and missing villi, decreased height and density of the mucosal layer, and significant interstitial atrophy, compared to the intestines of young rats. After MSCs treatment, the aforementioned aging-related tissue

manifestations were significantly improved, and the HE staining results of vital organs in the treatment group rats were similar to those in the young group rats (Fig. 2-A/B/C). Immunohistochemical staining results indicated significant deposition of p16 and p21 in the lung, kidney, and intestinal tissues of naturally aging rats, which were notably reduced in area following treatment with MSCs (Fig. 2-A/B/C). Correspondingly, there was a significant reduction in the H-Score (Fig. 2-D/E/F).

As classic aging-related factors, the levels of  $\beta$ -gal and lipofuscin in the lungs, kidneys, intestines, and peripheral blood significantly increased during aging. However, the levels of  $\beta$ -gal and lipofuscin in various organs and peripheral blood all significantly decreased in MSCs treatment group relative to aged rats (Fig. 3-A/B). In addition, oxidative stress-related factors SOD, MDA, and GSH are closely related to organism aging. This study found that, compared with young rats, the levels of

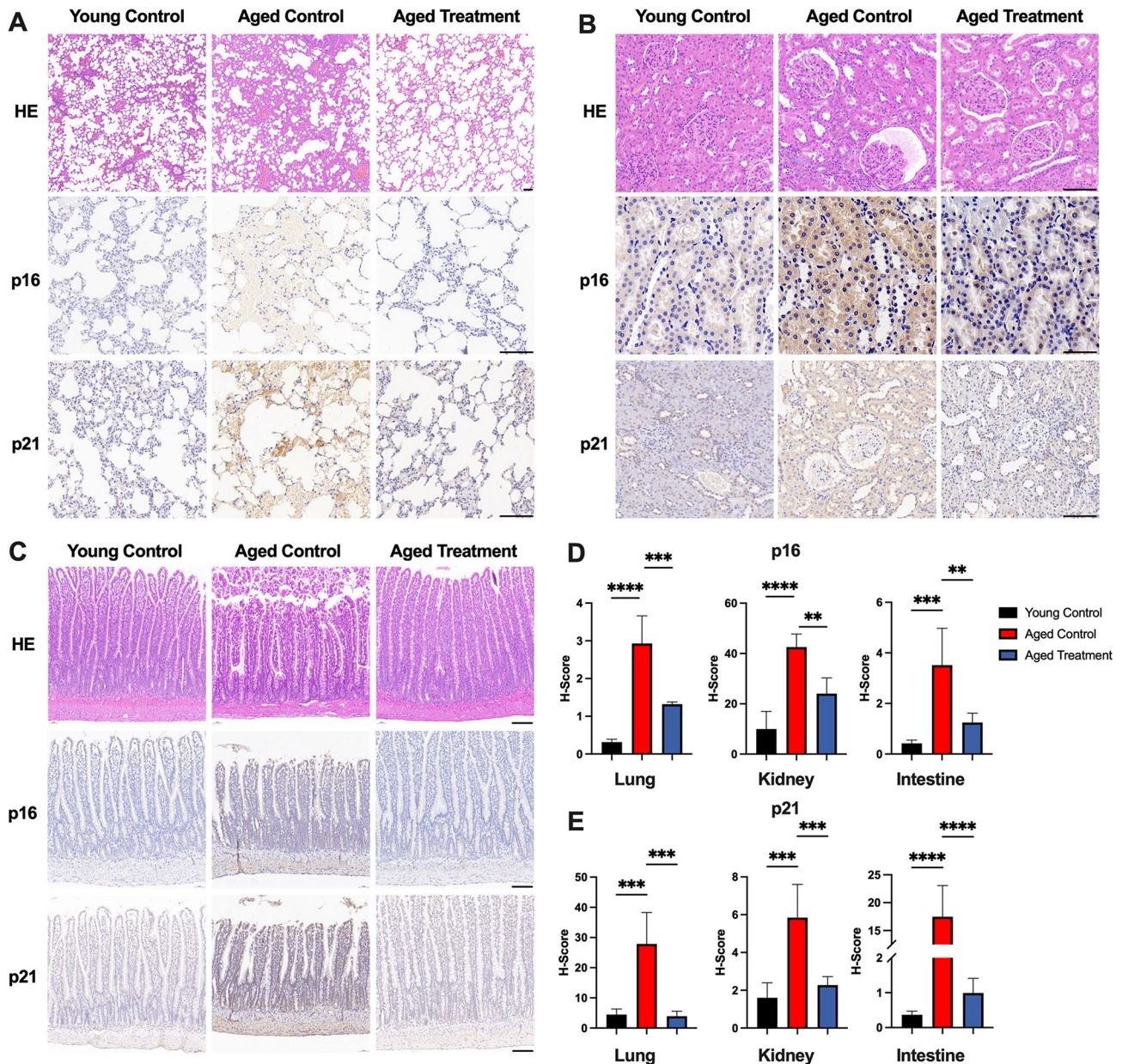


**Fig. 2** HE Staining and Immunohistochemical Staining for p16 and p21 in the Lungs, Kidneys and Small Intestine. **(A)** HE staining, along with p16 and p21 immunohistochemical staining, in the pulmonary tissues of various rat groups, scale bar = 100  $\mu$ m. **(B)** HE staining, complemented by p16 and p21 immunohistochemical staining, in the renal tissues of different rat cohorts, scale bar = 100  $\mu$ m. **(C)** HE staining and immunohistochemical analyses for p16 and p21 in the intestinal tissues of various rat groups, scale bar = 100  $\mu$ m. **(D)** Scoring of p16 and p21 immunohistochemical staining in lung tissues ( $n=5$ ). **(E)** Scoring of p16 and p21 immunohistochemical staining in renal tissues ( $n=5$ ). **(F)** Scoring of p16 and p21 immunohistochemical staining in intestinal tissues ( $n=5$ ).  $**p < 0.01$ ,  $***p < 0.001$ ,  $****p < 0.0001$

SOD in the organs and peripheral blood of old rats significantly decreased, and the levels of MDA significantly increased. Yet, after MSCs treatment, the levels of SOD in the organs and peripheral blood of the treatment group rats significantly increased, and the levels of MDA significantly decreased compared to aged control group. While the changes in GSH levels in different organs and peripheral blood of old rats varied compared to young rats. Interestingly, however, GSH levels were increased in all organs in the aged treatment group compared to the aged control group, with statistically significant differences in the lungs, intestines, and peripheral blood (Fig. 3-C/D/E). The results of the detection of aging-related factors in various organs suggest that, compared with young rats, the levels of IgG in the organs and peripheral blood of old rats decreased, and the differences in the lungs, kidneys, and peripheral blood were statistically significant. However, IgG levels in lungs, kidneys, and peripheral blood were significantly higher in the aged treatment group of rats compared to aged rats (Fig. 3-F). Elevated levels of IL-1 $\beta$  and IL-6 were observed in the lungs, kidneys, and peripheral blood of aged rats compared to young rats. Compared with aged control rats, IL-1 $\beta$  and IL-6 levels were significantly decreased in lungs and kidneys of aged rats after MSCs treatment, whereas the differences in intestines and peripheral blood were not statistically significant (Fig. 3-G/H/I/J). These results suggest that in aging rats, aging-related factors such as  $\beta$ -gal, Lipo, p16, and p21 are significantly increased in peripheral vital organs like the lungs, kidneys, and intestines, along with a marked increase in oxidative stress and the presence of chronic inflammation and tissue structural disarray in some organs. Following MSCs infusion, these aging-related alterations showed significant amelioration.

#### Anti-aging effects of MSCs on central nervous system

The results of brain cortex HE staining revealed that, compared with young rats, the cerebral cortex of old rats exhibited a significant decrease in the number of neurons, accompanied by cell volume shrinkage, coagulation, and rounding of residual cells, resulting in lighter staining. However, after MSCs treatment, the number of neurons in the cerebral cortex of old rats increased, with a neat arrangement, clear structure, and normal staining (Fig. 4-A). Additionally, the results of Nissl staining in the hippocampus area showed significant changes in the morphology and structure of pyramidal cells in old rats. These changes were characterized by loose and disordered arrangement, a decrease in the number of Nissl bodies, and cell deformation and nuclear coagulation. Following MSCs treatment, the morphology and structure of cells in the hippocampus area substantially improved. The cells were evenly arranged, with clear outlines, decreased numbers of deformed cells, and an

increased number of Nissl bodies compared to old rats (Fig. 4-B/E). Compared to young rats, there was no significant increase in the levels of IL-1 $\beta$  and IL-6 in the brain tissues of aged rats. Following treatment with MSCs, these levels decreased, but without statistical significance. Immunohistochemical results suggest a notable increase in the deposition of p16 and p21 in the brain tissues of aging rats. Post-treatment with MSCs, there was a significant reduction in the positive area of p16 and p21 in the brain tissues (Fig. 4-C/D/F/G). Furthermore, in the brain tissue of old rats, the levels of  $\beta$ -gal, lipofuscin, and MDA significantly increased compared to young rats, but after MSCs treatment, these levels decreased significantly, with statistically significant differences observed. Moreover, MSCs treatment increased the levels of SOD, GSH, and IgG in the brain tissue of old rats, approaching the levels found in young rats. Levels of IL-1 $\beta$  and IL-6 in the brain tissues of different groups of rats did not exhibit statistically significant differences (Fig. 4-H). These results indicate that aging leads to a reduction in the number of neurons in rats, along with a significant increase in aging-related factors and oxidative stress levels. Treatment with MSCs can restore neuron numbers and reduce the levels of aging-related factors and oxidative stress.

#### Regulatory effect of MSCs on immune aging

The results of spleen HE staining revealed that, compared with young rats, the spleen tissue structure of old rats exhibited disorder, with mixed red and white pulp and unclear boundaries. There was a decrease in the number of spleen cells, and a loose arrangement, along with significant proliferation of spleen trabeculae and increased coarse fibers in the red pulp. However, after MSCs treatment, the proportion of white pulp in the spleen of old rats increased, the number of spleen cells increased, and the structural disorder was significantly improved (Fig. 5-A). Furthermore, TUNEL staining results indicated that, compared with young rats, there was a significant increase in the apoptosis of spleen cells in the spleen of old rats, which significantly improved after MSCs treatment (Fig. 5-B/F). Additionally, PCNA staining results suggested that the PCNA positivity rate of cells in the spleen of old rats was significantly lower than that of young rats. However, after MSCs treatment, the PCNA positivity rate of the spleen in old rats significantly increased, approaching the level of young rats (Fig. 5-C/G). Immunohistochemical results suggest that MSCs can significantly reduce the deposition of aging-related p16 and p21 in the spleen tissue (Fig. 5-D/E/H). Moreover, flow cytometry detection of CD4 $^+$ T cells and CD8 $^+$ T cells showed that, compared with young rats, the proportion of CD4 $^+$ T cells in the spleen of old rats significantly decreased, leading to a significant decrease

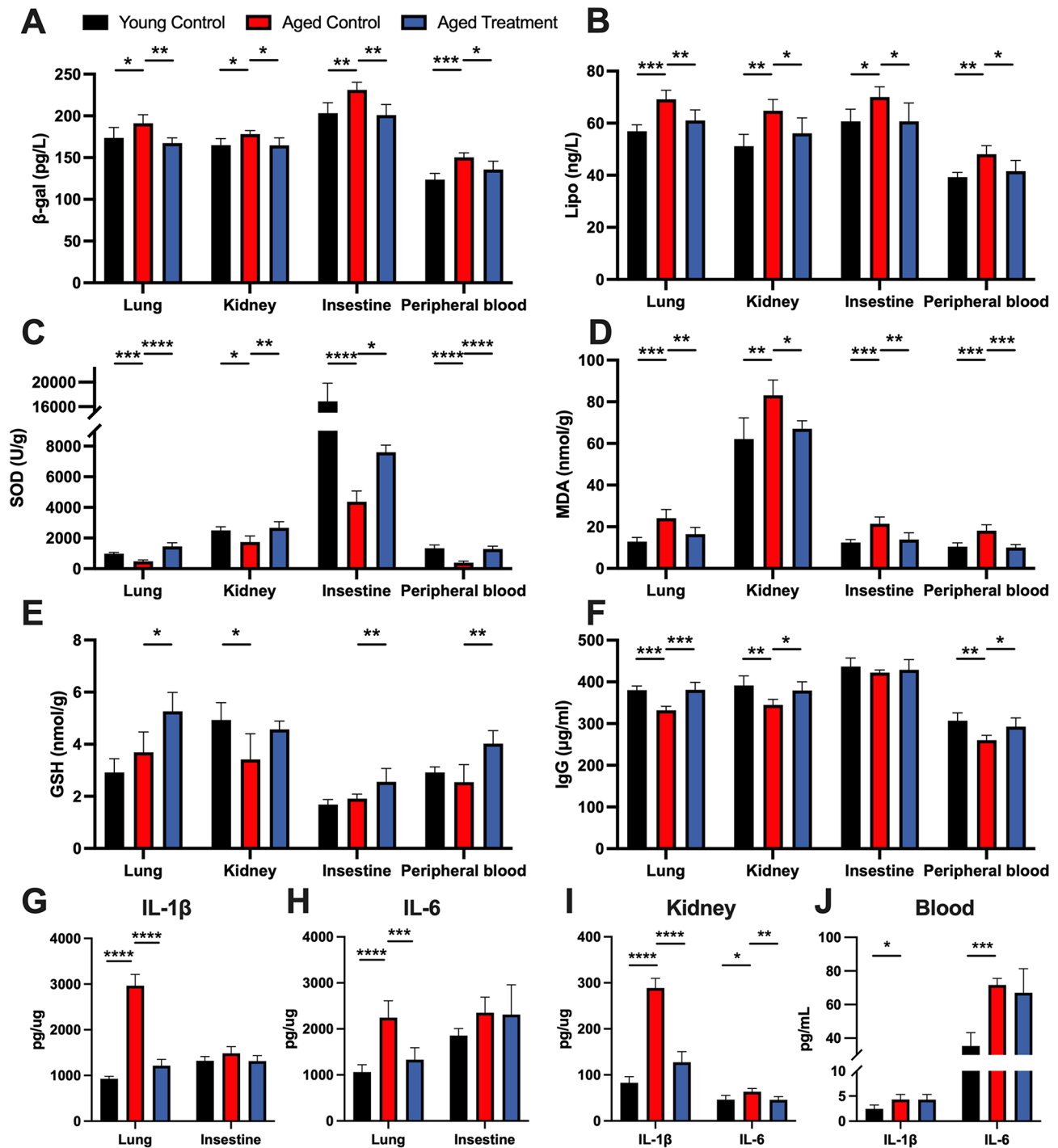


**Fig. 3** Levels of Aging-Related Biomarkers in the Lungs, Kidneys, Intestines, and Peripheral Blood of Different Rat Groups. **(A)**  $\beta$ -gal levels in the lungs, kidneys, intestines, and peripheral blood across various rat groups ( $n=5$ ). **(B)** Lipofuscin concentrations in the pulmonary, renal, intestinal, and peripheral blood specimens of different rat cohorts ( $n=5$ ). **(C)** SOD levels in the lungs, kidneys, intestines, and peripheral blood among the rat groups ( $n=5$ ). **(D)** MDA concentrations in the pulmonary, renal, intestinal, and peripheral blood samples across different rat cohorts ( $n=5$ ). **(E)** GSH levels in the lungs, kidneys, intestines, and peripheral blood in various rat groups ( $n=5$ ). **(F)** IgG concentrations in the lungs, kidneys, intestines, and peripheral blood of the rat groups ( $n=5$ ). **(G)** IL-1 $\beta$  levels in the pulmonary and intestinal tissues of different rat cohorts ( $n=5$ ). **(H)** IL-6 concentrations in the lungs and intestines among various rat groups ( $n=5$ ). **(I)** Levels of IL-1 $\beta$  and IL-6 in the renal tissues of the rat cohorts ( $n=5$ ). **(J)** Levels of IL-1 $\beta$  and IL-6 in the peripheral blood of different rat groups ( $n=5$ ). \* $p < 0.05$ , \*\* $p < 0.01$ , \*\*\* $p < 0.001$ , \*\*\*\* $p < 0.0001$



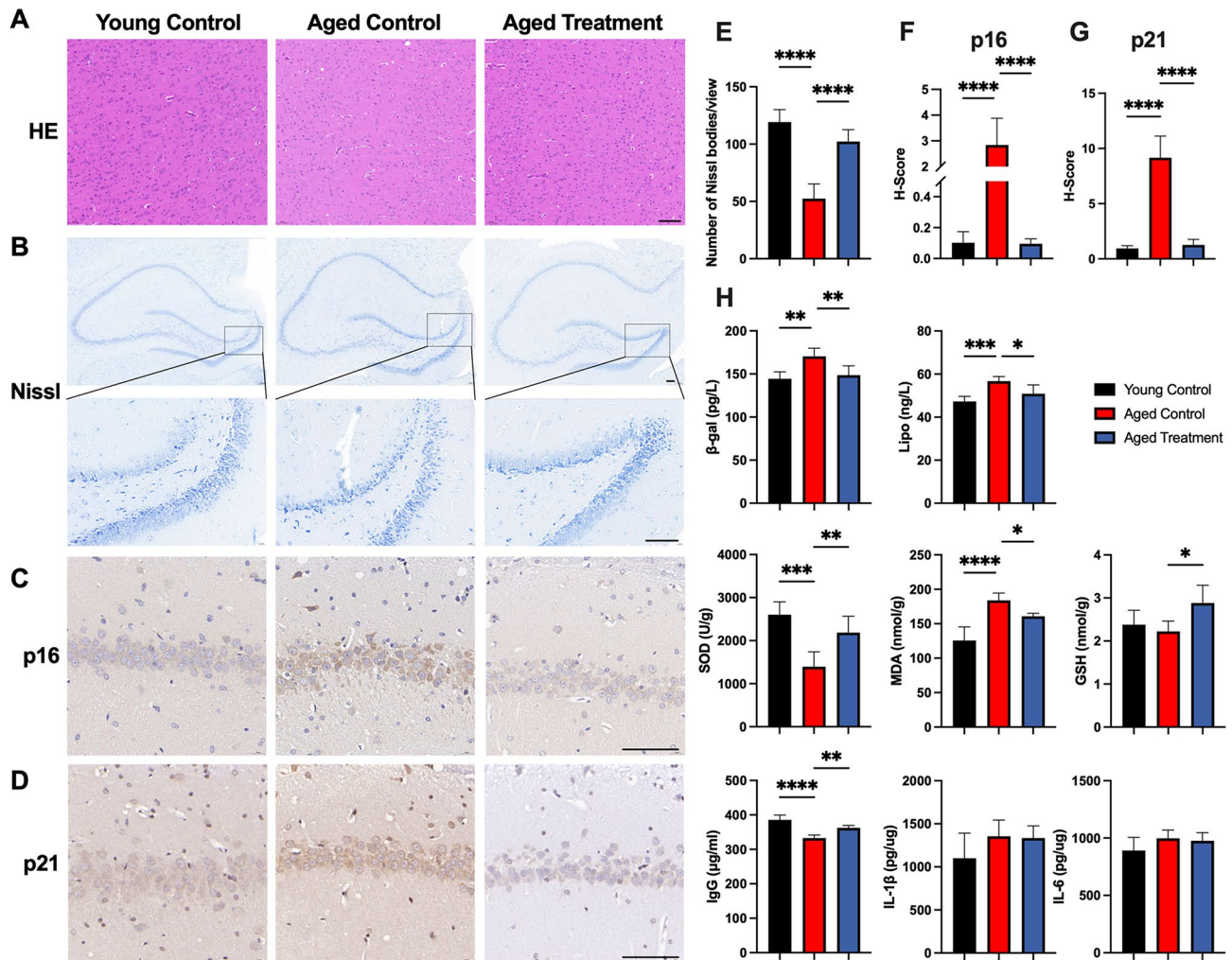


**Fig. 4** Staining of Rat Brain Tissues and Levels of Aging-Related Factors. **(A)** HE staining of the cerebral cortex in different rat groups, scale bar = 100  $\mu$ m. **(B)** Nissl staining of the hippocampal region of various rat cohorts, scale bar = 100  $\mu$ m. **(C)** Immunohistochemical staining for p16 in the hippocampal region of different rat groups, scale bar = 100  $\mu$ m. **(D)** Immunohistochemical staining for p21 in the hippocampal area of various rat cohorts, scale bar = 100  $\mu$ m. **(E)** Semi-quantitative analysis of Nissl staining in the hippocampal region ( $n=5$ ). **(F)** Immunohistochemical scoring for p16 in the hippocampus ( $n=5$ ). **(G)** Scoring of p21 immunohistochemistry in the hippocampal region ( $n=5$ ). **(H)** Levels of aging-related factors in brain tissues of different rat groups, including  $\beta$ -gal, lipofuscin, SOD, MDA, GSH, IgG, IL-1 $\beta$ , and IL-6 ( $n=5$ ). \* $p < 0.05$ , \*\* $p < 0.01$ , \*\*\* $p < 0.001$ , \*\*\*\* $p < 0.0001$

in the CD4+T/CD8+T ratio. Nevertheless, after MSCs treatment, the proportion of CD4+T cells significantly increased, the proportion of CD8+T cells significantly decreased, and the CD4+T/CD8+T ratio also significantly increased (Fig. 5-I/J). Additionally, in the spleen tissue of old rats, the levels of  $\beta$ -gal, lipofuscin, and MDA significantly increased compared to young rats, but all of these levels significantly decreased after MSCs treatment, approaching the levels observed in young rats. The level of SOD in the spleen tissue of old rats was significantly lower than that of young rats, and MSCs treatment could significantly increase the levels of SOD, GSH, and IgG in the spleen of old rats. In aged rats, compared to adults, there was no significant increase in IL-1 $\beta$  levels in the spleen, while IL-6 levels were notably elevated. Following treatment with MSCs, the levels of IL-6 were

significantly lower than those in the aged control group (Fig. 5-K). These results indicate a decline in immune function in aged rats, characterized by increased apoptosis in spleen cells, disordered tissue structure, a significant rise in aging-related factors and oxidative stress levels, and a reduced CD4+T/CD8+T cell ratio. After MSCs treatment, the aging-related immune phenotypes in aged rats showed significant improvement.

#### MSCs ameliorate lipid deposition and aging in the liver

The results of Oil Red O staining revealed that, compared with young rats, hepatocytes in the liver tissue of old rats showed disordered structure, with swollen cells and a large amount of red lipid deposition and lipid droplets in the cytoplasm, indicating obvious fatty degeneration. However, after MSCs treatment, the red lipid droplets

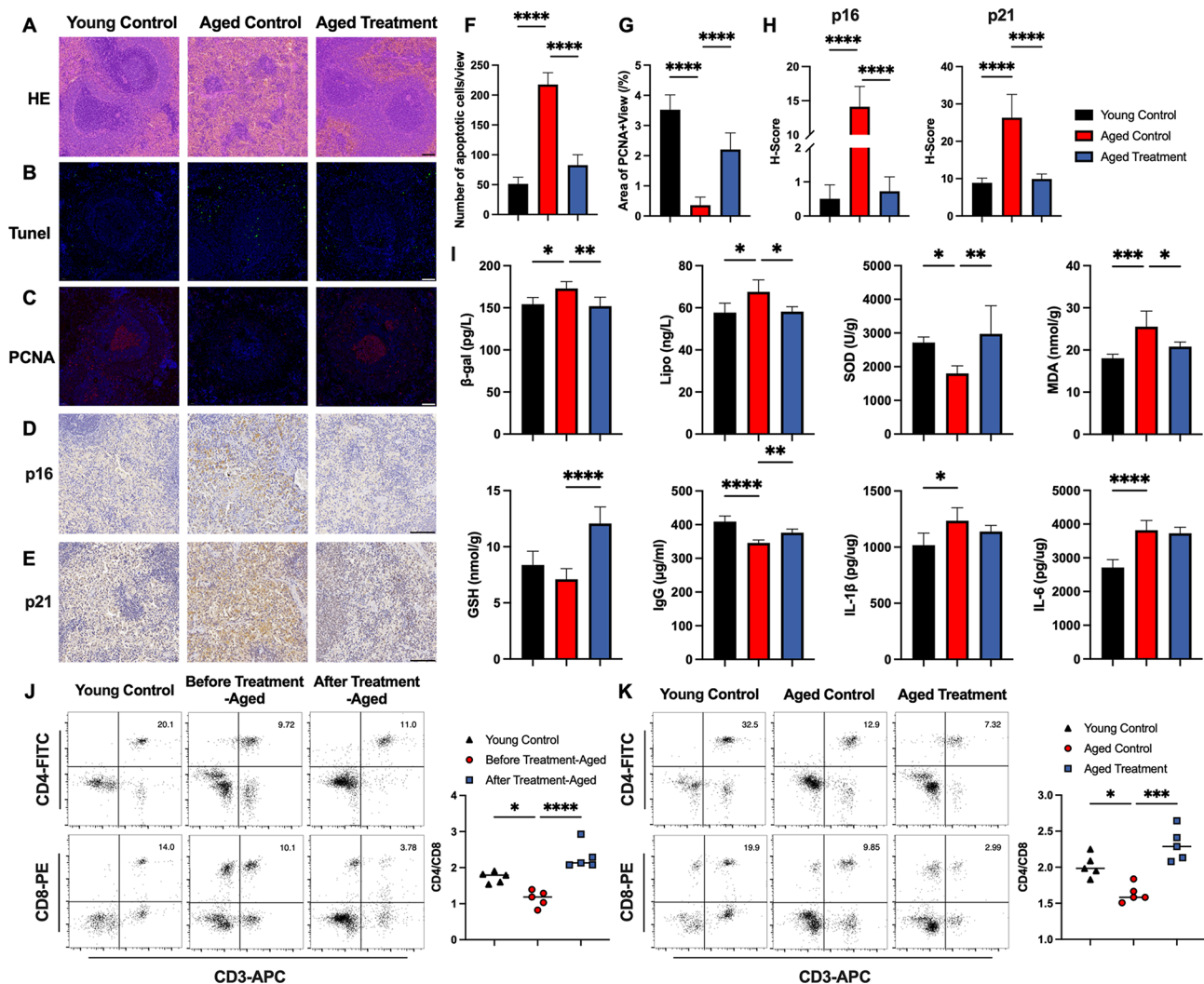


**Fig. 5** Spleen Staining, Levels of Aging-Related Factors in the Spleen, and Peripheral Blood CD4+T/CD8+T Ratio in Different Rat Groups. (A) HE staining of the spleen in various rat groups, scale bar = 100  $\mu$ m. (B) TUNEL staining of the spleen in different rat cohorts, scale bar = 100  $\mu$ m. (C) PCNA staining of the spleen in various rat groups, scale bar = 100  $\mu$ m. (D) Immunohistochemical staining for p16 in the spleens of different rat cohorts, scale bar = 100  $\mu$ m. (E) Immunohistochemical staining for p21 in the spleen across various rat groups, scale bar = 100  $\mu$ m. (F) Semi-quantitative analysis of TUNEL staining in the spleen ( $n=5$ ). (G) Semi-quantitative analysis of PCNA staining in the spleen ( $n=5$ ). (H) Immunohistochemical scoring for p16 and p21 in the spleen ( $n=5$ ). (I) CD4+T/CD8+T cell ratio in peripheral blood of young control group, aged treatment group pre-treatment, and aged treatment group post-treatment ( $n=5$ ). (J) CD4+T/CD8+T cell ratio in peripheral blood of different rat groups ( $n=5$ ). (K) Levels of aging-related factors in the spleen, including  $\beta$ -gal, lipofuscin, SOD, MDA, GSH, IgG, IL-1 $\beta$ , and IL-6 ( $n=5$ ). \* $p < 0.05$ , \*\* $p < 0.01$ , \*\*\* $p < 0.001$ , \*\*\*\* $p < 0.0001$

in the cytoplasm of hepatocytes significantly decreased in both size and number, leading to a significant reduction in the positive area of Oil Red O staining (Fig. 6-A/D). Immunohistochemical results indicate a substantial deposition of p16 and p21 in the liver tissues of aged rats. MSCs effectively reduce the intracellular levels and tissue deposition of p16 and p21 in the liver, as evidenced by a significant decrease in the H-Score (Fig. 6-B/C/E). Furthermore, compared with young rats, the levels of  $\beta$ -gal, lipofuscin, and MDA in the liver tissue of old rats significantly increased, but all of these levels decreased after MSCs treatment. The differences in  $\beta$ -gal and lipofuscin levels were statistically significant. Additionally,

the levels of SOD and IgG in the liver tissue of old rats were significantly lower than those of young rats. However, after MSCs treatment, the levels of SOD, GSH, and IgG in the liver of old rats significantly increased. Levels of IL-1 $\beta$  and IL-6 were significantly elevated in the liver tissues of aged rats. Post-treatment with MSCs, there was a marked reduction in IL-1 $\beta$  levels and a decrease in IL-6 levels, although the latter was not statistically significant (Fig. 6-F). These results suggest that MSCs can effectively ameliorate the aging phenotype of the liver, alleviating lipid deposition in the liver.

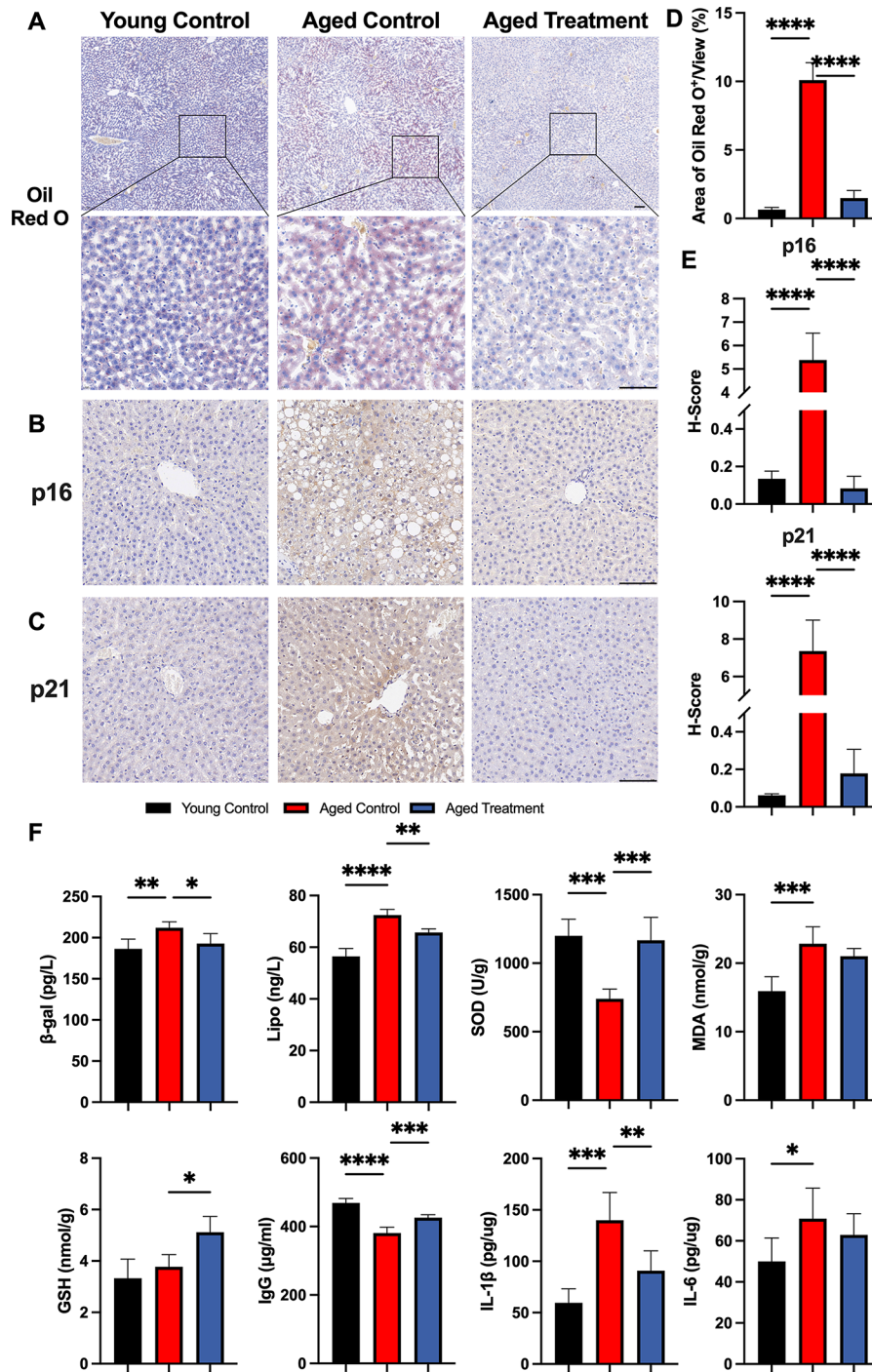


**Fig. 6** Liver Staining and Levels of Aging-Related Factors in Different Rat Groups. **(A)** Oil Red O staining of liver tissues in various rat groups, scale bar = 100  $\mu$ m. **(B)** Immunohistochemical staining for p16 in liver tissues of different rat cohorts, scale bar = 100  $\mu$ m. **(C)** Immunohistochemical staining for p21 in the liver of various rat groups, scale bar = 100  $\mu$ m. **(D)** Semi-quantitative analysis of Oil Red O staining in liver tissues ( $n=5$ ). **(E)** Immunohistochemical scoring for p16 and p21 in the liver ( $n=5$ ). **(F)** Levels of aging-related factors in the liver, including  $\beta$ -gal, lipofuscin, SOD, MDA, GSH, IgG, IL-1 $\beta$ , and IL-6 ( $n=5$ ). \* $p < 0.05$ , \*\* $p < 0.01$ , \*\*\* $p < 0.001$ , \*\*\*\* $p < 0.0001$

### Improvement effect of MSCs on myocardial aging-related injury

The results of Oil Red O staining indicated that, compared with young rats, there was a substantial amount of lipid accumulation in the myocardial tissue of old rats. The cytoplasmic lipid red staining became significantly deeper, indicating an increase in cellular lipid content. However, after MSCs treatment, the lipid accumulation in the myocardial tissue of old rats significantly decreased, approaching the level observed in young rats (Fig. 7-A/G). The results of Masson staining showed that, compared with young rats, the shape of myocardial cells in old rats was irregular, and there was disordered arrangement. Additionally, a considerable amount of collagen fibers accumulated in the interstitium of myocardial cells. However, after MSCs treatment, the fibrotic area in the interstitium of myocardial cells significantly

decreased, suggesting an improvement in the fibrotic condition (Fig. 7-B/H). Furthermore, the results of WGA staining revealed that, compared with young rats, the myocardial cells of old rats exhibited significant hypertrophy and disarray. Nevertheless, after MSCs treatment, there was an improvement in the hypertrophy of myocardial cells (Fig. 7-C/I). Immunohistochemical results indicate a substantial deposition of p16 and p21 in the cardiac tissues of aging rats. Treatment with MSCs can reduce the accumulation of these aging factors in the heart, as evidenced by a significant decrease in the H-Score (Fig. 7-D/E/F). These results demonstrate that MSCs effectively alleviate lipid deposition in the heart and liver caused by aging, improve myocardial fibrosis and cardiomyocyte hypertrophy, and reduce the levels of aging-related factors and oxidative stress in liver tissue.

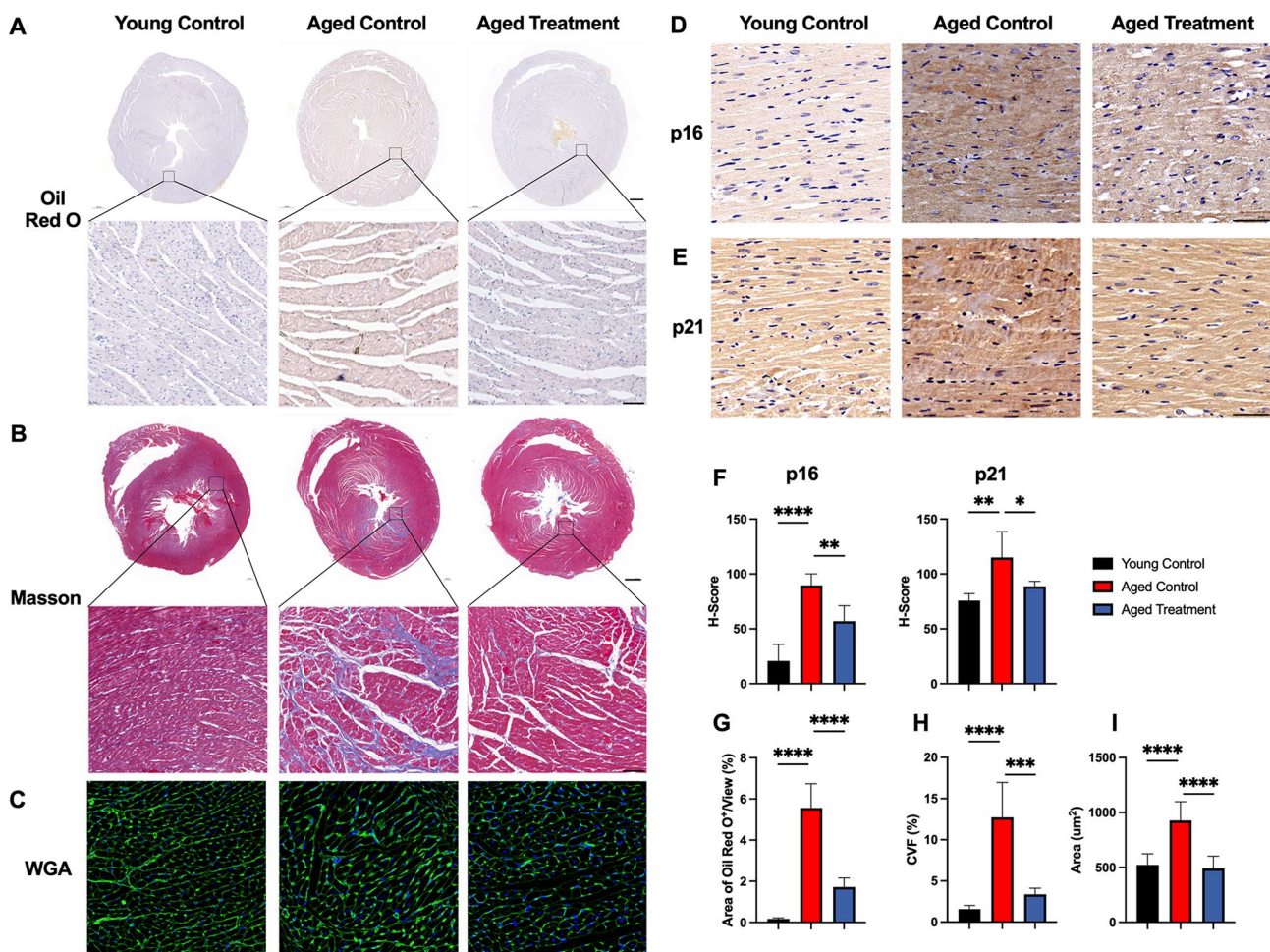


**Fig. 7** Cardiac Tissue Staining in Different Rat Groups. **(A)** Oil Red O staining of cardiac tissues, with the first row scale bar = 1000  $\mu\text{m}$  and the second row scale bar = 100  $\mu\text{m}$ . **(B)** Masson's trichrome staining of cardiac tissues, first row scale bar = 1000  $\mu\text{m}$ , second row scale bar = 100  $\mu\text{m}$ . **(C)** WGA staining of cardiac tissues, scale bar = 100  $\mu\text{m}$ . **(D)** Immunohistochemical staining for p16 in cardiac tissues, scale bar = 50  $\mu\text{m}$ . **(E)** Immunohistochemical staining for p21 in the heart, scale bar = 50  $\mu\text{m}$ . **(F)** Immunohistochemical scoring for p16 and p21 in cardiac tissues ( $n=5$ ). **(G)** Semi-quantitative analysis of Oil Red O staining in the heart ( $n=5$ ). **(H)** Quantification of myocardial collagen volume fraction in cardiac tissues ( $n=5$ ). **(I)** Cross-sectional area of cardiac myocytes ( $n=25$ ). \* $p < 0.05$ , \*\* $p < 0.01$ , \*\*\* $p < 0.001$ , \*\*\*\* $p < 0.0001$

**MSCs regulate aging-related changes in gut microbiota**

Principal Coordinates Analysis (PCoA) of species diversity revealed that, compared to the young control group, samples from the aged control and aged treatment groups are more closely clustered, indicating higher similarity among them (Fig. 8-A). The results of gut microbiota 16 S RNA analysis demonstrated that after MSCs treatment, there was an increase in the abundance of *Firmicutes*, *Bacteroidetes*, and *Proteobacteria* at the phylum level in old rats. Moreover, the composition of the

microbiota tended to resemble that of young rats (Fig. 8-B). At the species level, there was a significant increase in the abundance of *Prevotella\_9*, while the abundance of *Lachnospiraceae* decreased, indicating a certain improvement in the gut microbiota (Fig. 8-B). Analysis of relative bacterial abundance at the phylum level reveals that beneficial gut microbes such as *Verrucomicrobia*, *Firmicutes*, and *Actinobacteria* are the most abundant microbial taxa in the aged treatment group. This indicates that MSCs have improved the composition of the

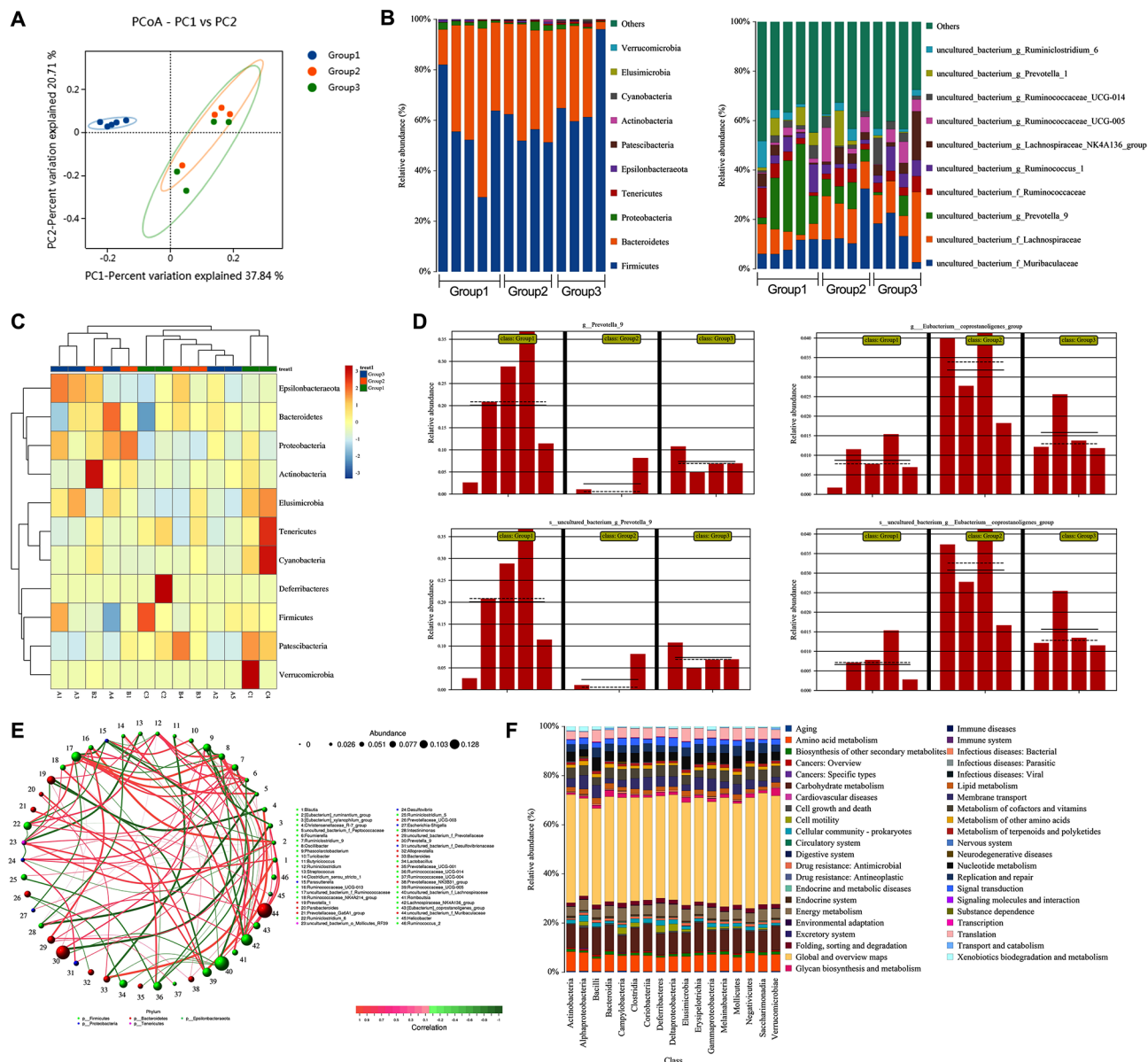


**Fig. 8** Intestinal Microbiota Composition and Changes in Different Rat Groups. (A) Principal Coordinate Analysis (PCoA) of the intestinal microbiota in various rat groups. (B) Relative abundance of microbial species at the phylum and genus levels in the intestinal microbiota of different rat cohorts. (C) Heatmap representing the abundance of microbial species at the phylum level across various rat groups. (D) Relative abundance of specific bacteria, such as *Prevotella* and *Coprococcus*, in different rat populations. (E) Network diagram of species at the genus level in the intestinal microbiota of various rat groups. (F) Prediction of gene types and abundance in the microbiota at the phylum level, integrating KEGG pathway information for different rat groups. Group1: Young control group; Group2: Aged control group; Group3: Aged treatment group

gut microbiota in aged rats (Fig. 8-C). These findings suggest that MSCs can partially restore the function of the gut microbiota in old rats. LEfSe analysis results revealed notable differences between the two genera in different treatments. The abundance of *Coprococcus*, a true rod-shaped bacterium, was significantly higher in aging rats, whereas *Prevotella* was significantly higher in young rat populations than in old rats. Notably, the proportion of these two bacteria in the aged rats treated with MSCs fell between the levels observed in young rats and naturally aging rats (Fig. 8-D). The species network diagram exhibited a strong correlation between *Prevotella* and *Furcellaria*, indicating a robust interaction between these two bacteria in the composition of the gut microbiota (Fig. 8-E). Finally, we employed the 16 S rRNA gene data from PICRUSt to analyze the functional gene composition of the microbiota at the phylum level. Differential analysis of KEGG metabolic pathway composition suggests that MSCs modulate the microenvironment within the intestines of aged rats primarily through pathways like amino acid metabolism, carbohydrate metabolism, metabolism of cofactors and vitamins, and energy metabolism (Fig. 8-F). These results indicate that aging leads to significant alterations in the gut microbiome of rats. MSCs can improve the composition of the microbiome, bringing it closer to the “younger state” seen in young rats. This may influence the physiological activities of other organs, potentially through the modulation of pathways such as amino acid and carbohydrate metabolism.

## Discussion

The primary objective of this study is to comprehensively investigate the anti-aging effects of MSCs on naturally aged rats and explore the potential regulatory mechanisms. Our findings reveal that MSCs transplantation significantly reduces the levels of aging-related factors and oxidative stress factors in multiple organs of naturally aged rats. Moreover, it improves chronic tissue damage and inflammatory states resulting from aging, reduces lipid deposition in the liver, and mitigates myocardial fibrosis. Furthermore, MSCs transplantation is shown to alleviate the decline in immune function and immune cell apoptosis associated with aging. Notably, our data also indicate that MSCs can positively modulate the composition of the gut microbiota in naturally aged rats. These results strongly suggest that MSCs transplantation therapy holds promise as a potentially effective anti-aging intervention, encompassing diverse aspects such as oxidative stress, tissue repair, metabolic regulation, and enhancement of immune function.

Contemporary medical perspectives strongly indicate that oxidative stress damage plays a pivotal role in organismal aging [20]. It adversely affects the cellular membrane structure, lipids, proteins, lipoproteins, and

DNA [21]. As a result, anti-aging research focuses on ameliorating the body's oxidative stress levels. Excessive production of free radicals can lead to lipid peroxidation, cell membrane and lipoprotein damage, and increased generation of MDA, which possesses significant cytotoxic and mutagenic properties, rendering it a classic biomarker for assessing oxidative stress [22]. Nonetheless, cells exert great effort to maintain their normal physiological functions, and the body's antioxidant defense system plays a critical role in eliminating surplus free radicals and reducing oxidative stress levels [23]. Studies have demonstrated that as the body ages and reactive oxygen species (ROS) levels increase, the entire antioxidant defense system becomes impacted. The activities of SOD and GSH markedly decrease, further aggravating ROS accumulation and oxidative stress damage [24]. In our study, we observed significantly increased levels of SOD and decreased levels of MDA and GSH in naturally aged rats, across various organs including blood, brain, lungs, kidneys, liver, intestines, and spleen. After MSCs treatment, the levels of MDA in aging rats significantly decreased, while the levels of SOD and GSH significantly increased. This indicates that MSCs can effectively ameliorate oxidative stress damage in aging rats and protect the body's antioxidant defense system. In a systematic review exploring the correlation between oxidative stress and extreme longevity, researchers found that compared to the aged control group, centenarians with extreme longevity exhibited significantly lower levels of MDA and significantly increased GSH activity [25]. Thus, MSCs have the ability to regulate the body's oxidative stress levels, enhance antioxidant enzyme activity, and their substantial antioxidant capacity highlights their robust potential for anti-aging purposes.

Oxidative stress can trigger an increase in aging-related  $\beta$ -galactosidase activity [26] and local tissue deposition of lipofuscin in cells [27], both of which are considered classic markers of aging. Moreover, elevated  $\beta$ -gal activity and Lipo deposition can severely disrupt the normal physiological activities of cells [28]. Since oxidative stress damage occurs throughout the body, aging affects cells, tissues, and organs simultaneously, albeit at varying rates across organs. In this study, we assessed the levels of  $\beta$ -gal and Lipo in peripheral blood and major organs. The results demonstrated that naturally aged rats exhibited varying degrees of increased  $\beta$ -gal and Lipo levels in different organs. Following MSCs treatment, the levels of these two markers significantly decreased, suggesting that MSCs have the potential to slow down the aging process in various organs. Brain aging can cause chronic mild inflammation, potentially linked to abnormal activation of microglial cells [29]. Additionally, aging is associated with brain atrophy, particularly in the prefrontal cortex and hippocampus [30], characterized by

increased neuronal death and decreased neurogenesis [31]. These changes are closely related to cognitive deficits, intellectual decline, sleep disorders, and circadian rhythm disruptions [32]. Our research found that MSCs treatment significantly improved chronic inflammation and neuronal apoptosis in the cerebral cortex of aging rats. Moreover, the arrangement of neurons in the hippocampus became more orderly, indicating that MSCs may play a positive role in delaying brain aging. Heart aging is often linked to hypertrophic growth and fibrosis of cardiomyocytes [33]. Telomere damage can activate the pro-aging pathways p21 and p16 in cardiomyocytes, leading to non-classical profibrotic and prohypertrophic aging-related secretory phenotypes [34]. Interestingly, clearing aged cardiomyocytes in mice can reverse cardiac fibrosis and cardiomyocyte hypertrophy processes [34]. Aged cardiomyocytes also exhibit specific microscopic features, such as the deposition of amyloid-like proteins and the accumulation of lipofuscin [35]. Our results indicated that MSCs infusion significantly improved cardiac fibrosis severity, to some extent alleviated cardiomyocyte hypertrophy, and ameliorated chronic myocardial inflammation and structural disorders associated with aging. This suggests that MSCs have a protective effect on heart aging. In summary, although aging occurs concurrently in all organs of the body, the anti-aging effect of MSCs is comprehensive. Evidence of MSC's anti-aging effects can be observed in each organ.

The incidence of metabolic syndrome increases with age, closely associated with obesity, hyperglycemia, abnormal blood lipids, insulin resistance, and cardiovascular disease. Particularly, excess visceral adipose tissue is linked to higher morbidity and metabolic imbalances [7]. Non-alcoholic fatty liver disease serves as a typical representative of metabolic syndrome, being the most common chronic liver ailment and a precursor to other aging-related diseases [36]. Our Oil Red O staining revealed significant lipid deposition in the liver and heart of naturally aged rats compared to young rats. During the experiment, we observed apparent obesity and significant thickening of subcutaneous fat in old rats. Prior research has shown that exosomes derived from UC-MSCs can ameliorate oxidative stress and lipid deposition in non-alcoholic steatohepatitis through the Nrf2/HO-1 signaling pathway [37, 38]. In our study, continuous MSCs injection alleviated lipid deposition in the liver and heart of aged rats, indicating that MSCs have a regulatory effect on aging-related lipid metabolism disorders. Recently, attention has been drawn to the close relationship between gut microbiota, metabolism, and aging. The microbial genome provides the host with greater genetic flexibility and environmental adaptability [39]. Increasing evidence highlights the role of gut microbiota composition in longevity [40, 41]. It has been observed

that compared with young individuals, aged individuals show decreased gut microbiota diversity with age [42], increased abundance of *Clostridium* and *Clostridium sporogenes* [43], and decreased abundance of *Lactobacillaceae*, *Pseudolactobacillaceae*, *Rikenellaceae*, and *Lactobacillaceae*. Moreover, researchers have found evidence of changes in intestinal permeability and chronic inflammation in aging mice [44]. Research has found that MSCs can modulate the homeostasis of the gut microbiome, thereby improving pathological changes in organs [45]. This includes conditions such as aortic atherosclerotic plaque [46] and Parkinson's disease [47]. Our study indicated that MSCs repaired damaged villous structures in the intestines of old rats and improved chronic inflammation. Furthermore, MSCs increased the diversity of intestinal flora and regulated the abundance of aging-related bacteria such as *Prevotella* and *Coprococcus*, suggesting that MSCs may rejuvenate the gut microbiota of old rats. Furthermore, the gut microbiome is also influenced by other organs, suggesting that the regulatory effects of MSCs on the gut microbiome are complementary to their anti-aging effects on other organs.

During the aging process, the immune system gradually loses its ability to effectively respond to pathogens and cancer cells, a condition known as "immunosenescence." This is characterized by changes in the ratio of naïve T cells and memory T cells, imbalanced CD4+T cells and CD8+T cells, impaired calcium-mediated signal transduction, and thymic atrophy [48]. Previous research has demonstrated that MSCs can improve immunosenescence through paracrine action and direct cell-to-cell contact, possibly by ameliorating aging-related chronic inflammation and inhibiting immune cell apoptosis [49]. In our study, we observed that naturally aging rats had a significantly reduced CD4+T/CD8+T ratio in peripheral blood, disordered splenic follicular structure, reduced quantity, a significant increase in the number of apoptotic cells in the spleen, and a decrease in the number of proliferating cells compared to young rats. However, after MSCs treatment, all these aging-related phenotypes in the naturally aging rats were significantly improved. Additionally, MSCs treatment led to reduced levels of  $\beta$ -gal, Lipo, and MDA in spleen tissue and increased SOD and GSH levels, indicating a protective effect of MSCs on spleen organ aging. Researchers have employed *Vac-iCre<sup>+/-</sup>; Erccl<sup>-fl</sup>* mice to establish an immunosenescence animal model. As these adult healthy mice aged, they exhibited exhaustion of specific immune cell groups and immune function impairment, which subsequently caused aging and damage of whole-body organs [50]. Hence, the immune system plays a crucial role in the overall aging process of the body. Considering the related results from our study, we have valid grounds to believe that MSCs can ameliorate the aging-related phenotypes

of multiple organs in the body, with the immunomodulatory effect of MSCs being one of the core mechanisms.

This investigation meticulously assessed various indicators within naturally aging animal models, including oxidative stress, senescence factors, immune senescence, lipid deposition, and gut microbiota, to scrutinize the progression of aging in several pivotal organs such as the heart, liver, and spleen. Compared to previous studies on the anti-aging properties of MSCs, the phenomena unveiled in this research are significantly more comprehensive and objective, indicating that MSCs can modulate the entire organism's aging process and achieve deceleration of aging through reciprocal interactions among different organs and systems. However, one noteworthy limitation of this research is the lack of profound exploration into the molecular mechanisms underlying MSCs' anti-aging effects. Moreover, due to the scarcity of naturally aging animals, a limited number of specimens were utilized in this study, hindering the implementation of a long-term observational study. Consequently, in subsequent investigations, we intend to employ a greater number of naturally aging animals and extended observational periods to delve into the anti-aging roles of exosomes derived from MSCs. Utilizing second and third-generation sequencing technologies, we aim to elucidate the molecular mechanisms and regulatory networks by which MSCs and their derivatives comprehensively delay organismal aging. In addition, the anti-aging effects of MSCs and their derivatives are worth trying, and this study provides some theoretical basis and potential direction for clinical research.

## Conclusion

This study provides a comprehensive confirmation of the anti-aging effects of MSCs on naturally aging rats. The transplantation of MSCs resulted in a significant reduction in aging-related and oxidative stress factors across multiple organs. It also alleviated chronic tissue damage and inflammation associated with aging, improved lipid deposition, myocardial fibrosis, and aging-induced alterations in gut microbiota. Furthermore, MSCs transplantation relieved aging-related immunodeficiency and immune cell apoptosis. These findings suggest that the anti-aging effects of MSCs encompass multiple aspects, including mitigation of oxidative stress, promotion of tissue repair, regulation of metabolism, and enhancement of immune function, thus presenting a promising anti-aging therapeutic approach.

## Abbreviations

MSCs	Mesenchymal stromal cells
rRNA	Ribosomal ribonucleic acid (rRNA)
UC-MSCs	Umbilical cord-derived mesenchymal stromal cells
MEM	Minimum essential medium
FBS	Fetal bovine serum
EDTA	Ethylenediaminetetraacetic acid

PBS	Phosphate buffered saline
HE	Hematoxylin-eosin
WGA	Wheat germ agglutinin
DAPI	4',6-diamidino-2-phenylindole
ELISA	Enzyme-linked immunosorbent assay
OD	Optical density
β-gal	Beta-galactosidase
Lipo	Lipofuscin
IgG	Immunoglobulin G
SOD	Superoxide dismutase
MDA	Malondialdehyde
GSH	Glutathione
DNA	Deoxyribonucleic acid
PCR	polymerase chain reaction
OTU	Operational taxonomic unit
ANOVA	One-way analysis of variance
IL	Interleukin
PCNA	Proliferating cell nuclear antigen
ROS	Reactive oxygen species

## Acknowledgements

Not applicable.

## Authors' contributions

W-L performed experiments, analyzed data, and wrote the manuscript. D-ZH and L-Y performed experiments and analyzed data. W-YQ and Y-RQ performed experiments. C-Y and W-M analyzed data. Z-FH revised the manuscript. Z-HY guided the experimental design and revised the manuscript. K-HJ designed and guided the experiments and revised the manuscript. All authors contributed to the article and approved the submitted version.

## Funding

This research was funded by The National Natural Science Foundation of China (No.62271506, No.61971441), the National Key R&D Program of China (Nos.2021YFC1005300, Nos.2021YFC1005302).

## Data availability

The datasets used and/or analyzed during the current study are available from the corresponding author on reasonable request.

## Declarations

### Ethics approval and consent to participate

This study was approved by The Ethics Committee of The Chinese PLA General Hospital, Beijing, China (No. 2017-X13-10).

### Consent for publication

Not applicable.

### Competing interests

The authors declared no competing interests.

### Author details

<sup>1</sup>Department of Critical Care Medicine, The First Medical Center, Chinese PLA General Hospital, 28 Fuxing Road, Haidian District, Beijing 100853, China

<sup>2</sup>Medical School of Chinese PLA, Beijing 100853, China

<sup>3</sup>National Key Laboratory of Kidney Diseases, Beijing Key Laboratory of Kidney Disease Research, National Clinical Research Center for Kidney Diseases, Beijing 100853, China

<sup>4</sup>Department of Basic Medicine, Graduate School, Chinese PLA General Hospital, Beijing 100853, China

<sup>5</sup>Department of General Surgery, The First Medical Center of Chinese PLA General Hospital, Beijing 100853, China

<sup>6</sup>Department of Emergency Medicine, The Second Hospital of Hebei Medical University, Shijiazhuang 050004, China

<sup>7</sup>Department of Nephrology, The First Medical Center of Chinese PLA General Hospital, 28 Fuxing Road, Haidian District, Beijing 100853, China

Received: 21 February 2024 / Accepted: 3 July 2024

Published online: 05 August 2024



## References

- Rosen RS, Yarmush ML. Current trends in anti-aging strategies. *Annu Rev Biomed Eng.* 2023;25:363–85.
- Singh P, Gollapalli K, Mangiola S, Schraner D, Yusuf MA, Chamoli M, Shi SL, Lopes Bastos B, Nair T, Riermeier A, et al. Taurine deficiency as a driver of aging. *Science.* 2023;380:eabn9257.
- Rea IM, Gibson DS, McGilligan V, McEnerlan SE, Alexander HD, Ross OA. Age and age-related diseases: role of inflammation triggers and cytokines. *Front Immunol.* 2018;9:586.
- Lemaitre JF, Moorad J, Gaillard JM, Maklakov AA, Nussey DH. A unified framework for evolutionary genetic and physiological theories of aging. *PLoS Biol.* 2024;22:e3002513.
- López-Otín C, Blasco MA, Partridge L, Serrano M, Kroemer G. The hallmarks of aging. *Cell.* 2013;153:1194–217.
- Prata C, Maraldi T, Angeloni C. Strategies to counteract oxidative stress and inflammation in chronic-degenerative diseases. *Int J Mol Sci.* 2022;23:6439.
- Amorim JA, Coppotelli G, Rolo AP, Palmeira CM, Ross JM, Sinclair DA. Mitochondrial and metabolic dysfunction in ageing and age-related diseases. *Nat Rev Endocrinol.* 2022;18:243–58.
- Borst J, Ahrends T, Bąbała N, Melief CJM, Kastenmüller W. CD4(+) T cell help in cancer immunology and immunotherapy. *Nat Rev Immunol.* 2018;18:635–47.
- Nadeeshani H, Li J, Ying T, Zhang B, Lu J. Nicotinamide mononucleotide (NMN) as an anti-aging health product - promises and safety concerns. *J Adv Res.* 2022;37:267–78.
- Yousefzadeh M, Hépita C, Vyas R, Soto-Palma C, Robbins P, Niedernhofer L. DNA damage-how and why we age? *Elife.* 2021;10:e62852.
- Galipeau J, Sensébé L. Mesenchymal stromal cells: clinical challenges and therapeutic opportunities. *Cell Stem Cell.* 2018;22:824–33.
- He Y, Chen D, Yang L, Hou Q, Ma H, Xu X. The therapeutic potential of bone marrow mesenchymal stem cells in premature ovarian failure. *Stem Cell Res Ther.* 2018;9:263.
- Wang L, Li Y, Xu M, Deng Z, Zhao Y, Yang M, Liu Y, Yuan R, Sun Y, Zhang H, et al. Regulation of inflammatory cytokine storms by mesenchymal stem cells. *Front Immunol.* 2021;12:726909.
- Xiao X, Xu M, Yu H, Wang L, Li X, Rak J, Wang S, Zhao RC. Mesenchymal stem cell-derived small extracellular vesicles mitigate oxidative stress-induced senescence in endothelial cells via regulation of miR-146a/Src. *Signal Transduct Target Ther.* 2021;6:354.
- Dorronsoro A, Santiago FE, Grassi D, Zhang T, Lai RC, McGowan SJ, Angelini L, Lavasani M, Corbo L, Lu A, et al. Mesenchymal stem cell-derived extracellular vesicles reduce senescence and extend health span in mouse models of aging. *Aging Cell.* 2021;20:e13337.
- Zhu Y, Ge J, Huang C, Liu H, Jiang H. Application of mesenchymal stem cell therapy for aging frailty: from mechanisms to therapeutics. *Theranostics.* 2021;11:5675–85.
- Wang L, Deng Z, Sun Y, Zhao Y, Li Y, Yang M, Yuan R, Liu Y, Qian Z, Zhou F, Kang H. The study on the regulation of Th cells by mesenchymal stem cells through the JAK-STAT signaling pathway to protect naturally aged Sepsis Model rats. *Front Immunol.* 2022;13:820685.
- Zhang Y, Deng Z, Li Y, Yuan R, Yang M, Zhao Y, Wang L, Zhou F, Kang H. Mesenchymal stem cells provide neuroprotection by regulating heat stroke-induced brain inflammation. *Front Neurol.* 2020;11:372.
- Dogan S, Vasudevaraja V, Xu B, Serrano J, Ptashkin RN, Jung HJ, Chiang S, Jungbluth AA, Cohen MA, Ganly I, et al. DNA methylation-based classification of sinonasal undifferentiated carcinoma. *Mod Pathol.* 2019;32:1447–59.
- Zhang Y, Zhao C, Zhang H, Chen M, Meng Y, Pan Y, Zhuang Q, Zhao M. Association between serum soluble alpha-klotho and bone mineral density (BMD) in middle-aged and older adults in the United States: a population-based cross-sectional study. *Aging Clin Exp Res.* 2023;35:2039–49.
- Hajam YA, Rani R, Ganie SY, Sheikh TA, Javaid D, Qadri SS, Pramodh S, Alsulmani A, Alkhanani MF, Harakeh S, et al. Oxidative stress in human pathology and aging: molecular mechanisms and perspectives. *Cells.* 2022;11:552.
- Nishida N, Arizumi T, Takita M, Kitai S, Yada N, Hagiwara S, Inoue T, Minami Y, Ueshima K, Sakurai T, Kudo M. Reactive oxygen species induce epigenetic instability through the formation of 8-hydroxydeoxyguanosine in human hepatocarcinogenesis. *Dig Dis.* 2013;31:459–66.
- Kaluderac N, Mialet-Perez J, Paolucci N, Parini A, Di Lisa F. Monoamine oxidases as sources of oxidants in the heart. *J Mol Cell Cardiol.* 2014;73:34–42.
- Vatner SF, Zhang J, Oydanich M, Berkman T, Naftalovich R, Vatner DE. Healthful aging mediated by inhibition of oxidative stress. *Ageing Res Rev.* 2020;64:101194.
- Belenguer-Varea Á, Tarazona-Santabalbina FJ, Avellana-Zaragoza JA, Martínez-Reig M, Mas-Bargues C, Inglés M. Oxidative stress and exceptional human longevity: systematic review. *Free Radic Biol Med.* 2020;149:51–63.
- Zhang L, Zhao J, Mu X, McGowan SJ, Angelini L, O'Kelly RD, Yousefzadeh MJ, Sakamoto A, Aversa Z, LeBrasseur NK, et al. Novel small molecule inhibition of IKK/NF- $\kappa$ B activation reduces markers of senescence and improves healthspan in mouse models of aging. *Aging Cell.* 2021;20:e13486.
- Pan C, Banerjee K, Lehmann GL, Almeida D, Hajjar KA, Benedicto I, Jiang Z, Radu RA, Thompson DH, Rodriguez-Boulán E, Nociari MM. Lipofuscin causes atypical necroptosis through lysosomal membrane permeabilization. *Proc Natl Acad Sci USA.* 2021;118:e2100122118.
- Liu X, Belmonte JCI, Zhang W, Liu GH. A  $\beta$ -galactosidase kiss of death for senescent cells. *Cell Res.* 2020;30:556–7.
- Baker DJ, Petersen RC. Cellular senescence in brain aging and neurodegenerative diseases: evidence and perspectives. *J Clin Invest.* 2018;128:1208–16.
- Wang Y, Du W, Hu X, Yu X, Guo C, Jin X, Wang W. Targeting the blood-brain barrier to delay aging-accompanied neurological diseases by modulating gut microbiota, circadian rhythms, and their interplays. *Acta Pharm Sin B.* 2023;13:4667–87.
- Seib DR, Martín-Villalba A. Neurogenesis in the normal ageing hippocampus: a mini-review. *Gerontology.* 2015;61:327–35.
- Satoh A, Imai SI, Guarente L. The brain, sirtuins, and ageing. *Nat Rev Neurosci.* 2017;18:362–74.
- Evangelou K, Vasileiou PVS, Papaspyropoulos A, Hazapis O, Petty R, Demaria M, Gorgoulis VG. Cellular senescence and cardiovascular diseases: moving to the heart of the problem. *Physiol Rev.* 2023;103:609–47.
- Anderson R, Lagnado A, Maggiorani D, Walaszczyk A, Dookun E, Chapman J, Birch J, Salmonowicz H, Ogrodnik M, Jurk D, et al. Length-independent telomere damage drives post-mitotic cardiomyocyte senescence. *EMBO J.* 2019;38:e100492.
- Lewis-McDougall FC, Ruchaya PJ, Domenjo-Vila E, Shin Teoh T, Prata L, Cottle BJ, Clark JE, Punjabi PP, Awad W, Torella D, et al. Aged-senescent cells contribute to impaired heart regeneration. *Aging Cell.* 2019;18:e12931.
- Chalasanani N, Younossi Z, Lavine JE, Charlton M, Cusi K, Rinella M, Harrison SA, Brunt EM, Sanyal AJ. The diagnosis and management of nonalcoholic fatty liver disease: practice guidance from the American Association for the study of liver diseases. *Hepatology.* 2018;67:328–57.
- Kang Y, Song Y, Luo Y, Song J, Li C, Yang S, Guo J, Yu J, Zhang X. Exosomes derived from human umbilical cord mesenchymal stem cells ameliorate experimental non-alcoholic steatohepatitis via Nrf2/NQO-1 pathway. *Free Radic Biol Med.* 2022;192:25–36.
- Shi Y, Yang X, Wang S, Wu Y, Zheng L, Tang Y, Gao Y, Niu J. Human umbilical cord mesenchymal stromal cell-derived exosomes protect against MCD-induced NASH in a mouse model. *Stem Cell Res Ther.* 2022;13:517.
- Bana B, Cabreiro F. The microbiome and aging. *Annu Rev Genet.* 2019;53:239–61.
- Smith P, Willemsen D, Popkes M, Metge F, Gandiwa E, Reichard M, Valenzano DR. Regulation of life span by the gut microbiota in the short-lived African turquoise killifish. *Elife.* 2017;6:e27014.
- Han B, Sivaramakrishnan P, Lin CJ, Neve IAA, He J, Tay LWR, Sowa JN, Sizovs A, Du G, Wang J, et al. Microbial genetic composition tunes host longevity. *Cell.* 2017;169:1249–e12621213.
- Claesson MJ, Jeffery IB, Conde S, Power SE, O'Connor EM, Cusack S, Harris HM, Coakley M, Lakshminarayanan B, O'Sullivan O, et al. Gut microbiota composition correlates with diet and health in the elderly. *Nature.* 2012;488:178–84.
- Odamaki T, Kato K, Sugahara H, Hashikura N, Takahashi S, Xiao JZ, Abe F, Osawa R. Age-related changes in gut microbiota composition from newborn to centenarian: a cross-sectional study. *BMC Microbiol.* 2016;16:90.
- Thevaranjan N, Puchta A, Schulz C, Naidoo A, Szamosi JC, Verschoor CP, Loukov D, Schenck LP, Jury J, Foley KP, et al. Age-associated microbial dysbiosis promotes intestinal permeability, systemic inflammation, and macrophage dysfunction. *Cell Host Microbe.* 2017;21:455–e466454.
- Huang B, Gui M, An H, Shen J, Ye F, Ni Z, Zhan H, Che L, Lai Z, Zeng J, et al. Babao Dan alleviates gut immune and microbiota disorders while impacting the TLR4/MyD88/NF-small ka, cyrillicB pathway to attenuate 5-Fluorouracil-induced intestinal injury. *Biomed Pharmacother.* 2023;166:115387.
- Li Y, Shi G, Han Y, Shang H, Li H, Liang W, Zhao W, Bai L, Qin C. Therapeutic potential of human umbilical cord mesenchymal stem cells on aortic atherosclerotic plaque in a high-fat diet rabbit model. *Stem Cell Res Ther.* 2021;12:407.
- Pu Y, Wu Q, Zhang Q, Huang T, Wen J, Wei L, Hashimoto K, Liu Y. Mesenchymal stem-cell-derived microvesicles ameliorate MPTP-induced neurotoxicity

in mice: a role of the gut-microbiota-brain axis. *Psychopharmacology*. 2023;240:1103–18.

48. Goronzy JJ, Weyand CM. Understanding immunosenescence to improve responses to vaccines. *Nat Immunol*. 2013;14:428–36.
49. Yeo GEC, Ng MH, Nordin FB, Law JX. Potential of mesenchymal stem cells in the rejuvenation of the aging immune system. *Int J Mol Sci* 2021;22:5749.
50. Yousefzadeh MJ, Flores RR, Zhu Y, Schmiechen ZC, Brooks RW, Trussoni CE, Cui Y, Angelini L, Lee KA, McGowan SJ, et al. An aged immune system drives senescence and ageing of solid organs. *Nature*. 2021;594:100–5.

### **Publisher's Note**

Springer Nature remains neutral with regard to jurisdictional claims in published maps and institutional affiliations.